Water Harvesting Research, 2017, 2(1): 13-23
DOI: 10.22077/jwhr.2017.592
www.jwhr.birjand.ac.ir
P-ISSN: 2476-6976, E-ISSN: 2476-7603

Climate change impacts on spatial-temporal variations of reference evapotranspiration in Iran

Mahdi Delghandi [a*], Sanaz Joorabloo [b], Samad Emamgholizadeh[c]

[a] Assistant Professor, Agricultural Faculty, Shahrood University of Technology, Shahrood, Iran.

[b] Graduated M.S Student, Agricultural Faculty, Shahrood University of Technology, Shahrood, Iran.

[c] Associate Professor, Agricultural Faculty, Shahrood University of Technology, Shahrood, Iran.

[*] Corresponding author, E-mail address: delghandi@gmail.com

Received: 14 March 2017 / Accepted: 24 June 2017

Abstract

Global warming due to greenhouse effect is expected to cause major changes in climate of some regions. The change of climate is likely to have a profound effect on hydrological cycle. Evapotranspiration (ET, as the major component of hydrological cycle, will affect crop water requirement and future planning and management of water resources. This study was conducted to investigate climate change impacts on spatiotemporal pattern of reference evapotranspiration (ET_o) in Iran. To this purpose, using Hargreaves and Samani -formula and monthly meteorological data at 20 meteorological stations, ET_o was calculated for the historical period. ET_o was calculated for two future periods (2015-2045 and 2070-20799) from the outputs of 15 AOGCM models under three emission scenarios (A2, A1B, and B2). The spatial distribution of ET_o was interpreted by Inverse Distance Weighted Interpolation method. Results showed that Scenarios A2 and A1B predict the same increase in annual mean ET_o in both the future periods (5% and 15% for the first and the second future period, respectively), however in scenario B1, the amount of increase in ET_o in the first and the second future periods were determined as 3% and 9.4 %, respectively. Spatial variation of annual ET_o showed that the increase in ET_o in future periods will be decreased by moving from the Persian Gulf regions toward the Northern regions.

Keywords: *AOGCM models, change, Emission scenarios, Reference evapotranspiration.*

1. Introduction

Reference evapotranspiration (ET_o) is a key hydrological variable quantifying a major water loss from catchments, which can be used to calculate actual evapotranspiration (ET_a), schedule irrigation, and prepare input data for hydrological models. Irrigation water requirement basically represents the difference between crop water requirement and effective precipitation. The only factors affecting ET_o are climatic parameters, as water is abundantly available at the reference evapotranspiring surface (Allen et al., 1998). The first climatic parameter is air temperature. As temperatures increase, evapotranspiration also goes up. In recent years, human activities have induced increase in atmospheric carbon dioxide (CO_2) which leads to global warming and climate change (IPCC, 2001; IPCC, 2007). Each of the last three decades has been successively warmer at the surface of Earth than any preceding decade since 1850. Although the number of climate change mitigation policies have been recently increased, total Green House Gases (GHG) emissions have been continuously augmented from 1970 to 2010, with a maximum rate between 2000 and 2010 (IPCC, 2014).

To project the future changes in ET_o, GCMs (General Circulation Models) are often used to provide future climatic factors for estimating ET_o (Li et al., 2012). Due to the coarse spatial resolution of GCM outputs, downscaling techniques are used to obtain weather and climate information at a local scale from relatively coarse-resolution GCMs (Wilby and Dawson, 2007). Downscaling methods are divided into two categories of dynamic downscaling methods and statistical downscaling methods. Dynamic downscaling methods have higher computational cost and are strongly dependent on the boundary conditions induced by GCMs. On the other hand, statistical downscaling methods establish a statistical relationship between observations and large-scale variables, which is then used along with and based on GCM data to obtain local scale variables (Wang et al., 2013).

Some studies have been conducted to address temporal and spatial trends of evapotranspiration in different regions throughout the globe. For instance, Harmsen et al. (2009) estimate ET_o under climate change conditions for three locations by the Penman–Monteith method. Temperature data were statistically downscaled and evaluated using DOE/NCAR PCM global circulation model. Liu and Yang (2010) detected negative trends for actual evapotranspiration. Chaouche et al. (2010) analyzed evapotranspiration in a French Mediterranean region in the context of climate change and observed an increase in annual mean temperature and annual potential evapotranspiration. In another study, Dynamic downscaling methods were used to estimate future evapotranspiration with an RCM (Regional Circulation Model) - HadRM3P- in a Mediterranean area (Lovelli et al., 2010). Li et al. (2012) found that on the Loess Plateau of China the projected increase in reference evapotranspiration will be 4%, 7%, and 12% for three periods of 2011–2040, 2041–2070, and 2071–2099, respectively. Jun et al., (2012) used the Penman-Monteith formula and monthly meteorological data to explicit the impact of climate change on reference evapotranspiration. Serrat-Capdevila et al. (2011) predicted daily evapotranspiration rates from 2000 to 2100 using the Penman–Monteith equation and meteorological projections from the IPCC fourth assessment report climate model runs. Results indicated that atmospheric demand will be greater and lead to an increased reference crop evaporation. Results of Zhang et al. (2015) showed that annual mean ET_o had a significant declining trend at the rate of 1.29 mm per year from 1961 to 2012 due to climate change. Over 2000 to 2050, an overall reduction of annual precipitation of 39.1 ± 55.1 mm and an increase in air temperature of about 1.57 ± 0.27 °C (from 0.84 to 2.31 °C) were predicted for the Mediterranean region. The consequent increase of annual reference evapotranspiration is 92.3 ± 42.1 mm (Saadi at al., 2015). Calanca et al. (2006) studied the effect of climate change on the summertime evapotranspiration regime of three Alpine river basins. The results revealed a reduction in evapotranspiration which depends on altitude. Actual evapotranspiration was found to increase at high altitudes, but to decrease in low elevation areas. Other studies have also been conducted to address climate change impacts on evapotranspiration in different regions globally (e.g. King et al., 2015; Nam et al., 2015; Goyal, 2004; King, 2006).

Up to now, no spatial and temporal climate change impacts on ET_o have been reported in Iran. Furthermore, in most climate change impact studies, the uncertainty of AOGCM models and the greenhouse gases emission scenarios have not been considered. In the present paper, climate change impacts on ET_o are assessed considering the uncertainty of AOGCM models and the greenhouse gases emission scenarios. The objective of this study is to project the spatiotemporal changes in ET_o during 2016–2045 and 2070-2099 by means of statistical downscaling method. This information is helpful in understanding the present changes in eco-hydrology and reducing the adverse impacts of climate change on water resources and crop production in Iran.

2. Materials and Methods

Study Area

Iran has an area of 1,648,195 km^2 (636,372 sq mil) and lies between latitudes 24° and 40° N, and longitudes 44° and 64°E. the climate of Iran ranges from arid or semiarid, to subtropical along the Caspian coast and the northern forests. On the northern edge of country (the Caspian coastal plain) temperatures rarely fall below freezing point and the area remains humid during the rest of the year. Summer temperatures rarely exceed 29 °C. Annual precipitation is 680 mm in the eastern part of the plain and more than 1,700 mm (66.9 in) in the western part. To the west, settlements in the Zagros basin experience lower temperatures, severe winters with average daily temperatures below zero, and heavy snowfall. The eastern and central basins are arid, with less than 200 mm of rain and have occasional deserts. Average summer temperatures rarely exceed 38 °C. The coastal plains of the Persian Gulf and Gulf of Oman in southern Iran have mild winters and very humid and hot summers. The annual precipitation ranges from 135 to 355 mm.

Evapotranspiration model

There are several models for estimating reference evapotranspiration (ET_o). Selecting a particular method for determining ET_o depends upon the type of meteorological data available for the given region and the accuracy desired in the computation of water needs (Goyal, 2004). Hargreaves and Samani (1985) developed a simplified equation for calculating ET_o, which only requires temperature, day of year, and latitude:

$$ET_o = 0.0135K_T(T + 17.78)(T_{max} - T_{min})^{0.5}R_a \quad (1)$$

Where, KT = empirical coefficient; Ra = extra-terrestrial radiation (mm/day); T_{max} = maximum daily temperature (°C); T_{min} =minimum daily temperature (°C); and T is the average daily temperature (°C). Since K_T usually assumes the value of 0.17, sometimes the 0.0135 K_T coefficients is replaced by 0.0023. The equation can also be used with R_a in MJ m-2 day^{-1}, by multiplying the right side of the equation by 0.408. This method (designated as HS in this paper) has produced good results, due to the fact that at least 80 percent of ET_o can be explained by temperature and solar radiation and ΔT is related to humidity and cloudiness (Samani and Pessarakli, 1986). Although this equation only needs a daily measurement of maximum and minimum temperatures, and is presented here as a temperature-based method, it effectively incorporates measurement of radiation indirectly. Therefore, in this study Hargreaves and Samani (HS) method was used for the determination of ET_o.

Data source

In this study, two sets of data, historical weather data (measured station data) and AOGCMs (Atmosphere – Ocean General Circulation Models) outputs, were used to calculate ET_o. Monthly observed T_{max} and T_{min} data (for the baseline period 1971–2000) of 20 selected synoptic meteorological stations (Table 1) distributed in the throughout Iran were obtained from the database of Iran Meteorological Organization.

Table 1. Characteristics of the studied synoptic meteorological stations

Station	Longitude	Latitude	T*	P*	Station	Longitude	Latitude	T*	P*
Bandar-abbas	49° 36′	27° 12′	27.2	136	Arak	49° 48′	34° 06′	11.8	316
Birjand	59° 18′	32° 54′	17	129	Kermanshah	47° 12′	34° 24′	13.3	437
Bushehr	50° 48′	29° 00′	24.2	216	Sanandaj	47° 00′	35° 18′	12.8	492
Bam	58° 21′	29° 06′	21.7	72	Shahrekord	50° 48′	32° 18′	12.1	266
Bandar-anzali	49° 28′	37° 28′	16.2	1853	Shiraz	52° 36′	29° 36′	16.8	316
Kerman	57° 00′	30° 18′	16	153	Tabriz	46° 12′	38° 06′	11.6	318
Sabzevar	57° 42′	36° 12′	16.1	169	Torbat heydariyeh	59° 12′	35° 18′	14.2	236
Semnan	53° 33′	35° 35′	18.2	139	Urmia	45° 06′	37° 42′	11.6	390
Tehran	51° 18′	35° 42′	16.4	220	Kashan	49° 28′	37° 28′	19.5	138
Yazd	54° 18′	31° 54′	18.9	55	Gorgan	54° 16′	36° 51′	13.4	511

*T and P are mean annual temperature and mean annual precipitation (mm), respectively.

As previously mentioned, AOGCMs are the most comprehensive tools for generating climatic parameters such as T_{max}, T_{min}, and precipitation. In the present study, outputs of 15 GCMs (Table 2) have been chosen. To this purpose, the SRES scenarios A1B, A2, and B1 for two 30-year periods, including 2016 to 2045 (2030) and 2070 to 2099 (2085), were used to examine how ET_o changes over future periods. Scenario A1B is based on a world with rapid economic growth and fast development of new technologies at a global scale. Scenario A2 refers to a world with regionally oriented economic growth. Finally, the B1 scenario depicts a globalized rapidly growing population with an ecologically friendly economy including the enforced introduction of clean and efficient technologies (IPCC, 2007). Delta Method was used for downscaling GCM outputs. The method is shown in the following equation:

$$T_i = T_{i,abs} + \Delta T \qquad (2)$$

Where, $T_{i,abs}$ indicates the observed temperature for the i^{th} month at in baseline period, T_i is temperature time series for i^{th} month in future period, ΔT is the long term monthly average temperature change which can be calculated as follows:

$$\Delta T = \bar{T}_{i,GCM,fut} - \bar{T}_{i,GCM,base} \qquad (3)$$

where, $\bar{T}_{i,GCM,fut}$ is the 30-year (e.g. 2016-2045) monthly average temperature for i^{th} month simulated by AOGCMs for the future periods (2016-2045 and 2070-2099), and $\bar{T}_{i,GCM,base}$ is the monthly average temperature for i^{th} month in the baseline period simulated by AOGCMs.

Table 2. characteristics of AOGCM models

Model	country	Atmosphere resolution	Ocean Resolution	Emission scenarios
BCM 2.0	Norway	T63 (9.1° × 9.1°) L31	0.5°–5.1° × 5.1° L35	A2, A1B, B1
CGCM3T63	Canada	T63 (~9.1° × 9.1°) L31	0.9° × 4.1° L29	A2, A1B, B1
CSIROM3.5	Australia	T63 (~9.1° × 9.1°) L18	0.8° × 9.1° L31	A2, A1B, B1
ECHO-G	Germany-Korea	T30 (~9.3° × 9.3°) L19	0.5°–8.2° × 8.2° L20	A2, A1B, B1
ECHAM5-OM	Germany	T63 (~9.1° × 9.1°) L31	1.5° × 5.1° L40	A2, A1B, B1
GFDLCM2.0	USA	2.0° × 5.2° L24	0.3°–0.1° × 0.1°	A2, A1B, B1
GISS-ER	USA	4° × 5° L20	4° × 5° L13	A2, A1B, B1
HADCM3	UK	2.5°×75.3° L19	1.25°×25.1°, L20	A2, A1B, B1
INMCM3.0	Russia	5° × 4° L21	2.5°×2°, L33	A2, A1B, B1
IPSLCM4	France	2.5° × 75.3° L19	2° × 2° L31	A2, A1B, B1
MIROC3.2 MEDRES	Japan	T106 (~1.1° × 1.1°) L56	0.2° × 3.0° L47	A2, A1B, B1
MRICGCM2.3.2 a	Japan	T42 (~8.2° × 8.2°) L30	0.5°–7.0° × 1.1° L40	A2, A1B, B1
NCAR-CCSM3	USA	T85 (4.1° × 4.1°) L26	0.3°–1° × 1° L40	A2, A1B, B1
NCARPCM	USA	T42 (4.1° × 4.1°) L26	0.3°–1° × 1° L40	A2, A1B, B1
CNRM-CM3	France	T42 L45	182×152L31	A2, A1B, B1

Spatial analysis of reference evapotranspiration

The IDW (Inverse Distance Weighted) interpolation method was used to interpret the spatial distribution of ET_o. Differences between the historical values of ET_o during 1971–2000 and the projected ET_o duringthe future periods were interpolated to show the future spatial changes of ET_o.

3. Results and Discussion

Mean monthly temperature changes

Using Eq (3), the temperature changes (ΔT) were calculated (2016-2045) and second future periods (2070-2099), for each AOGCM model and each month, under three emission scenarios A2, A1B, and B1. This process was carried out for all of the 20 cities. To investigate the temperature changes of Iran in the projected climate change, considering the existence of 15 AOGCM model, 20 cities, under each of the emissions scenarios, 300 data for ΔT, were selected. By averaging these 300 data, mean ΔTs of future periods and emission scenarios were determined. The results are illustrated in Fig. 1. Fig. 1, plots tempreture change diagrams of different scenarios for future periods. Each diagram relates to a future period and an emission scenario. The midpoint of each period (2025 and 2085) was used to show the future period.

As it can be seen in Fig. 1, mean temperature in Iran will increase during 2070-2099 more compared to the period 2016-2045. In the first future period, all three emission scenarios present relatively similar results. However, during the second future period, differences of scenarios are evident such that the highest increase in temperate occurs for scenario A2 and the lowest increase of temperature is for scenario B1. Scenario A1B also provides results between scenarios A2 and B1. It is obvious that the temperature increase will be higher in the warm months compared to the cold months.

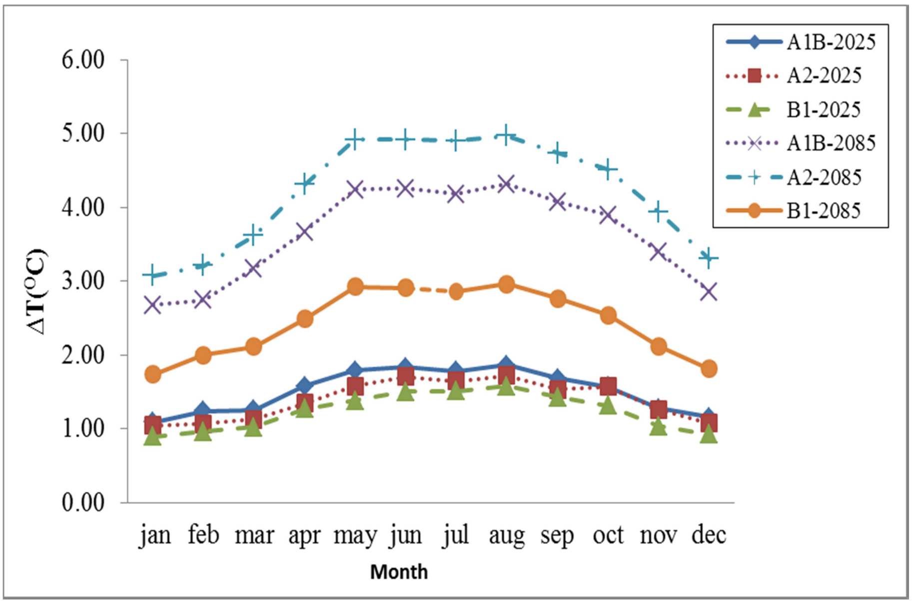

Fig. 1. The mean ΔT of the 20 synoptic meteorological stations in different scenarios.

Climate change Impact on ETo

After determining the values of ΔT for all 20 cities, monthly temperature scenarios for each six scenarios were calculated using Eq (1). For each scenario, ETo was calculated using Eq (1) for 30-year periods. Since it is recommended to designed irrigation systems with a probability of water requirement equal to 0.8 (Geerts et al., 2010), the present study also considered a probability of 0.8 (risk level of 0.2) in calculating mean ET_o. Thus one value was calculated for each city in each future period and each emission scenario. This process was carried out for the observed baseline period and monthly ET_o was determined for each city. During the next phase of the process, by averaging the results obtained for the 20 cities, mean ET_o of Iran was calculated at various scenarios and the baseline period (Fig. 2).

Fig. 2 shows an increase in ET_o for each of the two feature periods. Increase in ET_o is higher for 2070-2099 compared to the first period (2016-2045). In addition, it can be determined that all three scenarios of A1B, A2, and B1 represent similar results for the first future period. This is due to the near 1°C increase in temperature for all the three scenarios (Fig. 1). However, results of three emission scenarios differ during 2070-2099, such that scenarios A1B and B1 represent the greatest and the least increase in ET_o, respectively. Results of scenario A1B and A2 appear to be very close to each other, which was expected according to Fig. 1. But during the warm months, when the requirement and consequently the agricultural water demand are at their peak, scenario A2 shows the greatest increase in ET_o. Therefore, this scenario can be considered as the most critical scenario.

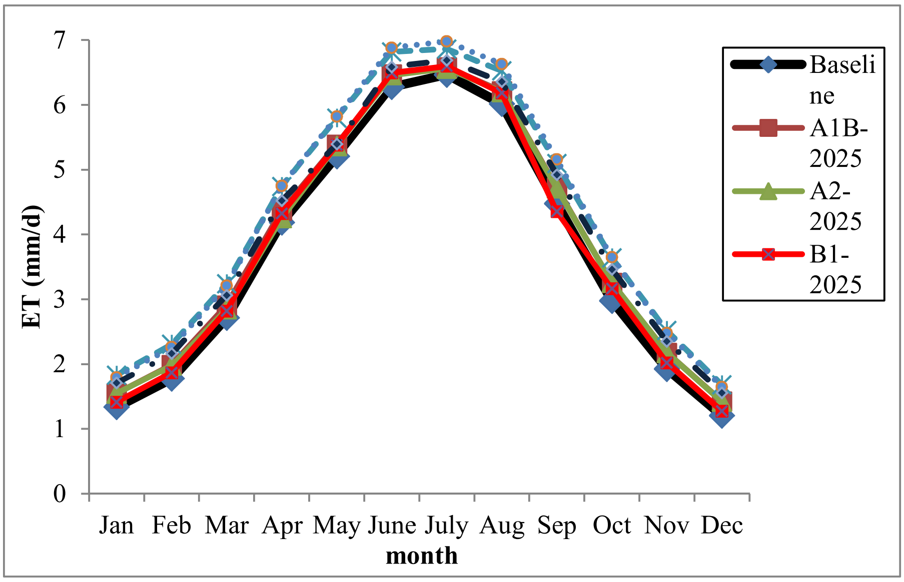

Fig. 2. The mean ET_o of Iran in all of the projected climate change scenarios and the baseline periods

Monthly and annual change percentages of ET_o for different scenarios are presented in Table 1. According to this table it can be determined that during the cold months, increase in percentage of ET_o is higher compared to the warm months (for various scenarios), so that the maximum increase in ET_o occurs in December for all of the six scenarios.

Table 1. Percentage differences between the historical values (1970–2000) and the projected ET_0 during 2016-2045 and 2071–2099

Scenarios	Month												annual
	Jan	Feb	Mar	Apr	May	June	July	Aug	Sep	Oct	Nov	Dec	
A1B-2030	15.8	11.7	7.0	4.3	3.4	3.1	1.8	3.2	5.5	9.3	12.9	18.3	5.5
A2-2030	15.8	11.2	4.9	1.6	3.1	2.9	1.5	3.1	5.3	9.4	12.9	18.0	5.0
B1-2030	5.8	5.0	3.9	3.3	3.3	3.5	2.0	2.8	-2.7	6.2	5.0	5.8	3.0
A1B-2085	36.8	29.6	19.4	13.2	11.3	8.6	6.1	8.4	13.8	22.2	30.7	39.3	14.5
A2-2085	34.3	27.1	18.2	13.4	11.7	9.6	7.9	10.2	15.2	22.4	28.9	36.7	15.0
B1-2085	27.7	21.6	12.8	8.0	3.6	4.9	3.4	5.7	10.0	16.3	22.2	29.0	9.4

The maximum increase in monthly ET_o was determined approximately by 18% (for both scenarios A2 and A1B), and 39% (in scenario A1B) in the first and the second future periods, respectively. According to Table 1 increase in annual ET_o for the first future period was calculated equal to 5.0, 5.5, and 3.0 percent for scenarios A2, A1B and B1, respectively. The corresponding values of 2070-2099 were 15, 14.5, and 9.4 percent.

As it was previously mentioned, scenario A2 can be considered as the most critical scenario in terms of agricultural water resources management. Therefore, for future changes in spatial pattern, the authors of this study mainly focus on scenario A2. Also as a mean of brevity, differences between the historical values and the projected ET_o during 2016-2045 and 2071–2099 are interpolated to show the spatial variations (Figs. 3 and 4).

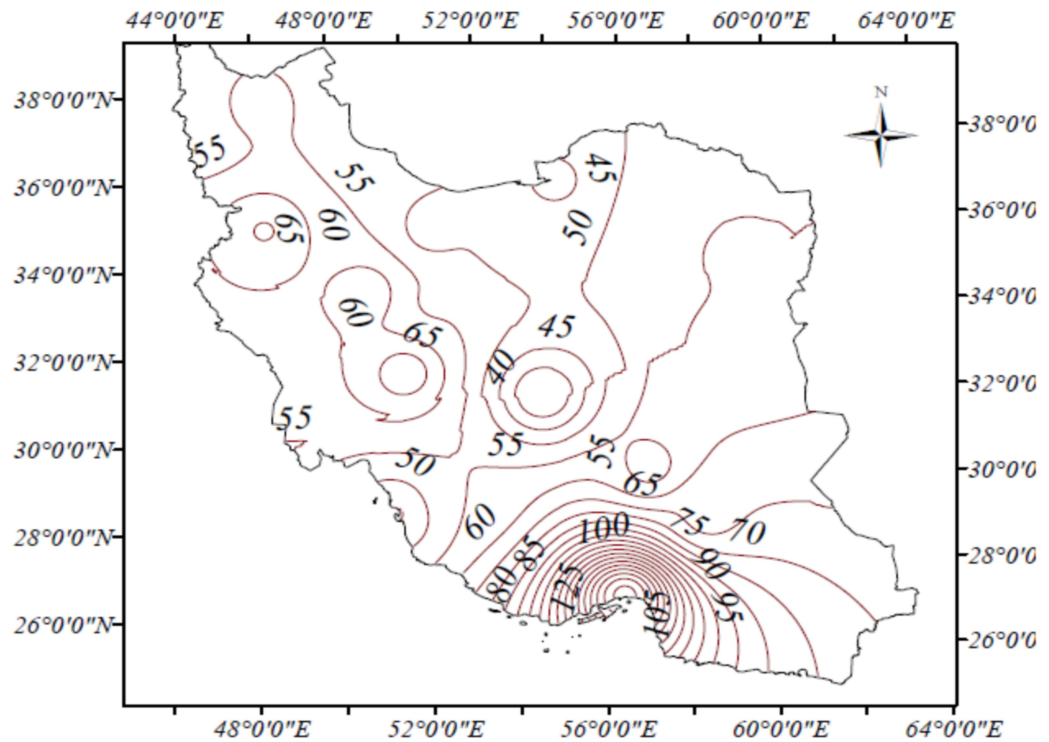

Fig. 3. The differences between the historical values and the projected ET_o during 2016-2045

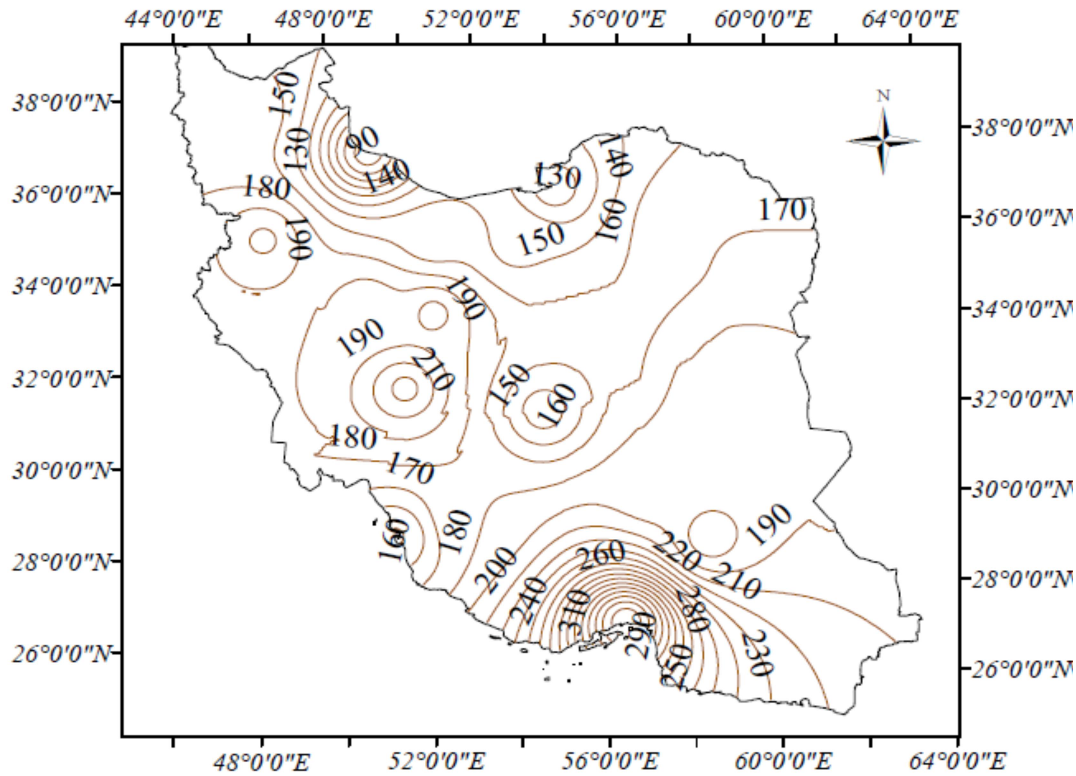

Fig. 4. The differences between the historical values and the projected ET_o during 2071–2099

According to Figs. 3 and 4, the greatest increase in annual ET_o in future periods occurs in southern regions of Iran (Persian Gulf littoral). By moving toward north, the increase in annual ET_o is reduced. Maximum and minimum increase in annual ET_o in the first future period were observed in Hormozgan province (about 120 mm) and the central Iran (about 40 mm), respectively. Meanwhile, in other regions of Iran, increase in annual ET_o was predicted between 50 and 65 mm. However, increase in annual ET_o will be higher in the second future period. The range of annual ET_o changes will be about 100 mm (in Gilan province) to 300 mm (in Hormozgah province) with ANT value from 150 mm up to 200 mm in other regions. ET_o value will increase in both of the future periods, compared to the base period.

4. Conclusion

The present and future spatiotemporal patterns of reference evapotranspiration (ET_o) were calculated in this paper in order to understand climate change impacts on ET_o in Iran. To this purpose, using Hargreaves and Samani formula and monthly meteorological data at 20 meteorological stations, ET_os were calculated. ET_os during two future periods (2015-2045 and 2070-20799) were calculated from 15 AOGCM models outputs under three emission scenarios (A2, A1B and B2). Spatial distribution of ET_o was interpreted by Inverse Distance Weighted Interpolation method. Climate change scenarios projected an upward trend in ET_0 for the 21st century; averaged across the two scenarios for the whole area, ET0 would increase by 4%, 7%, and 12% during 2020s, 2050s and 2080s, respectively. ET0 would continue increasing in the 21st century. Results showed that the increase in ET_o will be higher during 2070-2099 compared to the first period (2016-2045). The increase in the annual ET_o for the first future period equalled 5.0, 5.5, and 3.0 percent for scenarios A2, A1B and B1, respectively. These values were 15, 14.5, and 9.4 percent for the 2070-2099 period. It was determined that the increase percent in ET_o was higher in the cold months compared to the warm months (for various scenarios), with the maximum increase in ET_o occurring in December for all of the scenarios. Spatial variation of annual ET_o showed that the increase in ET_o in the future periods will decrease by moving from the Persian Gulf regions to the northern regions. The maximum and minimum increase in the annual ET_o in the first future period were observed in Hormozgan province (about 120 mm) and the central Iran (about 40 mm), respectively. Meanwhile, in other regions of Iran, the increase in annual ET_o was predicted between 50 and 65 mm. However, in the second future period, the increase in annual ET_o was predicted to be greater. The changing range of annual ET_o was predicted between 100 mm (in Gilan province) to 300 mm (in Hormozgah province) with ANT between 150 mm up to 200 mm for the other regions.

5. References

Allen, R.G., Pereira, L.S., Raes, D., & Smith, M. (1998). Crop evapotranspiration: guidelines for computing crop water requirements. FAO Irrigation and Drainage Paper No. 56, Rome.

Calanca, P., Roesch, A., Jasper, K., & Wild, M. (2006). Global warming and the summertime evapotranspiration regime of the Alpine region. Climatic Change, 79, 65–78.

Chaouche, K., Neppel, L., Dieulin, C., Pujol, N., Ladouche, B., Martin, E., Salas, D., &

Caballero, Y. (2010). Analyses of precipitation, temperature and evapotranspiration in a French Mediterranean region in the context of climate change. Comptes Rendus Geosciences, 342, 234–243.

Goyal, R.K. (2004). Sensitivity of evapotranspiration to global warming: A case study of arid zone of Rajasthan (India). Agricultural Water Management, 69, 1-11.

Harmsen, E. W., Miller, N.L., Schlegel, N.J., & Gonzalez, J.E. (2009). Seasonal climate change impacts on evapotranspiration, precipitation deficit and crop yield in Puerto Rico. Agricultural Water Management. 96, 1085-1095.

IPCC. Climate Change. (2001). In: Houghton, J. T., Ding, Y., Griggs, D.J., Noguer, M., van der Linden, P.J., Dai, X., Maskell, K., & Johnson, C.A. (Eds.). The Scientific Basis. Contribution of Working Group I to the Third Assessment Report of the Intergovernmental Panel on Climate Change. Cambridge University Press. 2001; 881 pp.

IPCC. Climate Change. (2007). The Physical Science Basis – Summary for Policy Makers. Contribution of Working Group I to the Fourth Assessment Report of the Intergovernmental Panel on Climate Change. Released February, 2007; 21 pp.

IPCC. Climate Change. (2014). Synthesis Report. Contribution of Working Groups I, II and III to the Fifth Assessment Report of the Intergovernmental Panel on Climate Change [Core Writing Team, Pachauri, R.K., & Meyer, L.A. (eds.)]. IPCC, Geneva, Switzerland, 151 pp.

Jun, W., Xinhua, W., Meihua, G., Xu, X. (2012). Impact of Climate Change on Reference Crop Evapotranspiration in Chuxiong City, Yunnan Province Procedia Earth and Planetary Science, 5, 113 – 119.

Kang, S., Kimball, J.S., & Running, S.W. (2006). Simulating effects of fire disturbance and climate change on boreal forest productivity and evapotranspiration. Science of the Total Environment. 362, 85–102.

King, D. A., Bacheleta, D. M., Symstad, A. J., K. F., & Hobbins, M. (2015). Estimation of potential evapotranspiration from extraterrestrial radiation, air temperature and humidity to assess future climate change effects on the vegetation of the Northern Great Plains, USA. Ecological Modelling, 297, 86–97.

Li, Z., Zheng, F. L., & Liu, W. Z. (2012). Spatiotemporal characteristics of reference evapotranspiration during 1961–2009 and its projected changes during 2011–2099 on the Loess Plateau of China. Agricultural and Forest Meteorology, 154, 147-155.

Liu, Q., & Yang, Z. (2010). Quantitative estimation of the impact of climate change on actual evapotranspiration in the Yellow River Basin, China. Journal of Hydrology, 395(3), 226-234.

Lovelli, S., Perniola, M., Di Tommaso, T., Ventrella, D., Moriondo, M., & Amato, M. (2010). Effects of rising atmospheric CO 2 on crop evapotranspiration in a Mediterranean area. Agricultural water management, 97(9), 1287-1292.

Nam, W. H., Hong, E. M., & Choi, J. Y. (2015). Has climate change already affected the spatial distribution and temporal trends of reference evapotranspiration in South Korea?. Agricultural Water Management, 150, 129–138.

Saadi, S., Todorovic, M., Tanasijevic, L., Pereira, L. S., Pizzigalli, C., & Lionello, P. (2015). Climate change and Mediterranean agriculture: Impacts on winter wheat and tomato crop evapotranspiration, irrigation requirements and yield. Agricultural Water Management, 147, 103–115.

Samani, Z. A., & Pessarakli, M. (1986). Estimating potential crop evapotranspiration with minimum data in Arizona. Transactions of the ASAE, 29(2), 522-0524.

Serrat-Capdevila, A., Scott, R. L., Shuttleworth, W. J., & Valdés, J. B. (2011). Estimating evapotranspiration under warmer climates: Insights from a semi-arid riparian system. Journal of hydrology, 399(1), 1-11.

Wang, W.G., Xing, W.Q., Shao, Q.X., Yu, Z.B., Peng, S.Z., Yang, T., Yong, B., Taylor, J., & Singh, V.P. (2013). Changes in reference evapotranspiration across the Tibetan Plateau: Observations and future projections based on statistical downscaling. J. Geophys. Res. Atmos, 118 (10), 4049–4068.

Wilby, R.L., & Dawson, C.W. (2007). SDSM 4.2: A Decision Support Tool for the Assessment of Regional Climate Change Impacts, User Manual. Department of Geography, Lancaster University, Lancaster.

Wilby, R.L., Dawson, C.W., & Barrow, E.M. (2002). SDSM – a decision support tool for the assessment of regional climate change impacts. Environmental Modelling and Software, 17 (2), 145–157.

Zhang, K. X., Pan, S. M., Zhang, W., Xu, Y. H., Cao, L. G., Hao, Y. P., & Wang, Y. (2015). Influence of climate change on reference evapotranspiration and aridity index and their temporal-spatial variations in the Yellow River Basin, China, from 1961 to 2012. Quaternary International, 380, 75-82.